

Rational Analysis of Melting Point Behaviour of Co-crystals of 4-Nitrophenol with Some Aza-compounds

Amrita Nayak, and Venkateswara R. Pedireddi

Cryst. Growth Des., **Just Accepted Manuscript** • DOI: 10.1021/acs.cgd.6b01011 • Publication Date (Web): 07 Sep 2016

Downloaded from <http://pubs.acs.org> on September 8, 2016

Just Accepted

“Just Accepted” manuscripts have been peer-reviewed and accepted for publication. They are posted online prior to technical editing, formatting for publication and author proofing. The American Chemical Society provides “Just Accepted” as a free service to the research community to expedite the dissemination of scientific material as soon as possible after acceptance. “Just Accepted” manuscripts appear in full in PDF format accompanied by an HTML abstract. “Just Accepted” manuscripts have been fully peer reviewed, but should not be considered the official version of record. They are accessible to all readers and citable by the Digital Object Identifier (DOI®). “Just Accepted” is an optional service offered to authors. Therefore, the “Just Accepted” Web site may not include all articles that will be published in the journal. After a manuscript is technically edited and formatted, it will be removed from the “Just Accepted” Web site and published as an ASAP article. Note that technical editing may introduce minor changes to the manuscript text and/or graphics which could affect content, and all legal disclaimers and ethical guidelines that apply to the journal pertain. ACS cannot be held responsible for errors or consequences arising from the use of information contained in these “Just Accepted” manuscripts.



Rational Analysis of Melting Point Behaviour of Co-crystals of 4-Nitrophenol with Some Aza-compounds

Amrita Nayak* and V. R. Pedireddi

Solid State and Supramolecular Structural Chemistry Laboratory, School of Basic Sciences, Indian Institute of Technology Bhubaneswar, Bhubaneswar 751 007, India.

Email: amrita.nayak003@gmail.com

ABSTRACT

Various co-crystals of 4-nitrophenol with aza-compounds have been synthesized and characterized by single crystal X-ray diffraction method. Thermal analysis of all the co-crystals infers higher melting point compared to their respective co-formers and the increase in melting point perhaps because of the cross-chain close packed arrangement of the constituent molecules. The trend of increase in melting point among the co-crystals reported here is difficult to correlate because of the diverse nature of the aza-compounds. Therefore we have grouped the co-crystals based on the position of the nitrogen atom of aza-compounds. Apart from structural features the melting point trend among the co-crystals has also been correlated by considering the parameters such as crystal density, packing efficiency and number of strong hydrogen bonds. It has been noticed that within the group, the co-crystal with higher value of above said parameters shows higher melting point compared to the co-crystals with lower values, inferring a linear correlation between any of these parameters and the corresponding melting point of the co-crystal.

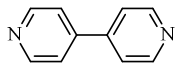
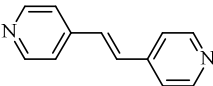
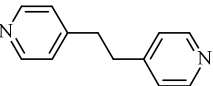
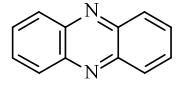
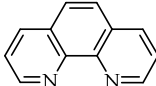
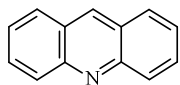
INTRODUCTION

Co-crystallization¹⁻⁸ is a viable supramolecular synthetic method to bring multiple molecular components into a crystal lattice and it is an amenable pathway for a molecular solid to get altered physicochemical properties.⁹⁻¹⁷ It is well documented that such physicochemical properties of molecular solids depend upon the type and strength of the intermolecular interactions present in the molecular ensembles.¹⁸⁻²⁷ Melting point is one of

1
2
3 the important physical property of a molecular solid which also could be varied *via* co-
4 crystallization process.²⁸⁻³¹ For instance, Braga *et al.*,³² reported the odd-even effect of
5 melting point behaviour of homologous aliphatic dicarboxylic acids in the co-crystals with
6 co-formers 1,2-bis(4-pyridyl)ethane and 1,3-bis(4-pyridyl)propane. The odd-even effect of
7 melting point is retained with respect to the total number of carbon atoms in the co-crystal.
8
9 However, Bond *et al.*,³³ showed reversed melting point behaviour in the co-crystals of
10 aliphatic dicarboxylic acids with pyrazine and this anomalous behaviour is explained based
11 on the density of co-crystals. Further, Veidis *et al.*,³⁴ explained melting point behaviour of co-
12 crystals of phenanthridine with various dicarboxylic acids based on the strength of the
13 intermolecular interactions apart from the crystal density.
14
15
16
17
18
19
20
21
22
23
24
25

26 It is to note that, in general, most of the co-crystals have melting point in between the
27 corresponding co-formers³⁵⁻⁴² and very few co-crystals have higher melting point than their
28 corresponding individual components⁴³⁻⁴⁴. In fact, the statistics given by Schultheiss *et al.*⁴⁵,
29 corroborate this fact, wherein out of 50 pharmaceutical co-crystals, only four have higher
30 melting point as compared to their co-formers. In addition, it is also interesting to note that
31 the co-crystals are being observed with higher melting points are mostly the molecular
32 complexes with carboxylic acid functional moieties. Thus, towards thrust for co-crystals with
33 higher melting points, engaging molecules with different functional groups other than
34 carboxylic acid, we have found seven co-crystals of 4-nitrophenol and different aza
35 compounds (Chart 1) with higher melting points.
36
37
38
39
40
41
42
43
44
45
46
47
48
49
50
51
52
53
54
55
56
57
58
59
60

Chart 1

			reactants	complex (composition)
 4-nitrophenol (1)			(1) + (a)	1a (2:1)
 4,4'-bipyridine (a)	 1,2-bis(4-pyridyl)ethene (b)	 1,2-bis(4-pyridyl)ethane (c)	(1) + (b)	1b (2:1)
 phenazine (d)	 Pyrazine (e)	 1,10-phenanthroline (f)	(1) + (c)	1c (2:1)
			(1) + (d)	1d (2:1)
			(1) + (e)	1e (2:1)
 Acridine (g)			(1) + (f)	1f (1:1)
			(1) + (g)	1g (1:1)

EXPERIMENTAL SECTION

All chemical reagents and solvents were obtained from commercial suppliers and used as received without any further purification. Highly pure spectroscopic grade solvents were used for all crystallization experiments. All molecular complexes **1a** – **1g** were prepared by dissolving the respective reactants in MeOH and allowing the solvent to evaporate under ambient conditions. In all cases good quality single crystals suitable for X-ray diffraction analysis were obtained.

In a typical co-crystallization experiment, 20 mg of 4-nitrophenol (0.145 mmol) and 26 mg 1,2-bis(4-pyridyl)ethane (0.145 mmol) were dissolved in 10 ml of MeOH in a 25 ml conical flask, by warming on a water bath. The resultant solution was allowed to evaporate under ambient conditions and single crystals were obtained over a period of 48-72 hrs.

Crystal structure determination

Good quality single crystals of **1a-1g** were carefully chosen after they were viewed under Leica microscope supported by a rotatable polarizing stage. The crystals were mounted on a goniometer by gluing to a glass fiber and crystal data were collected on a Bruker single-crystal X-ray diffractometer (D8 VENTURE) equipped with a PHOTON 100 CMOS detector. All the crystals were stable throughout the data collection and data collection was smooth. The structures were solved by intrinsic phasing method followed by full matrix least squares refinement against F^2 using SHELXTL and no anomalies were observed at any stage of structure solutions. All nonhydrogen atoms were refined anisotropically and hydrogen atoms were either refined or placed in calculated positions. The intermolecular interactions were computed using PLATON⁴⁶ or Mercury⁴⁷ software. The packing diagrams were generated using Diamond⁴⁸.

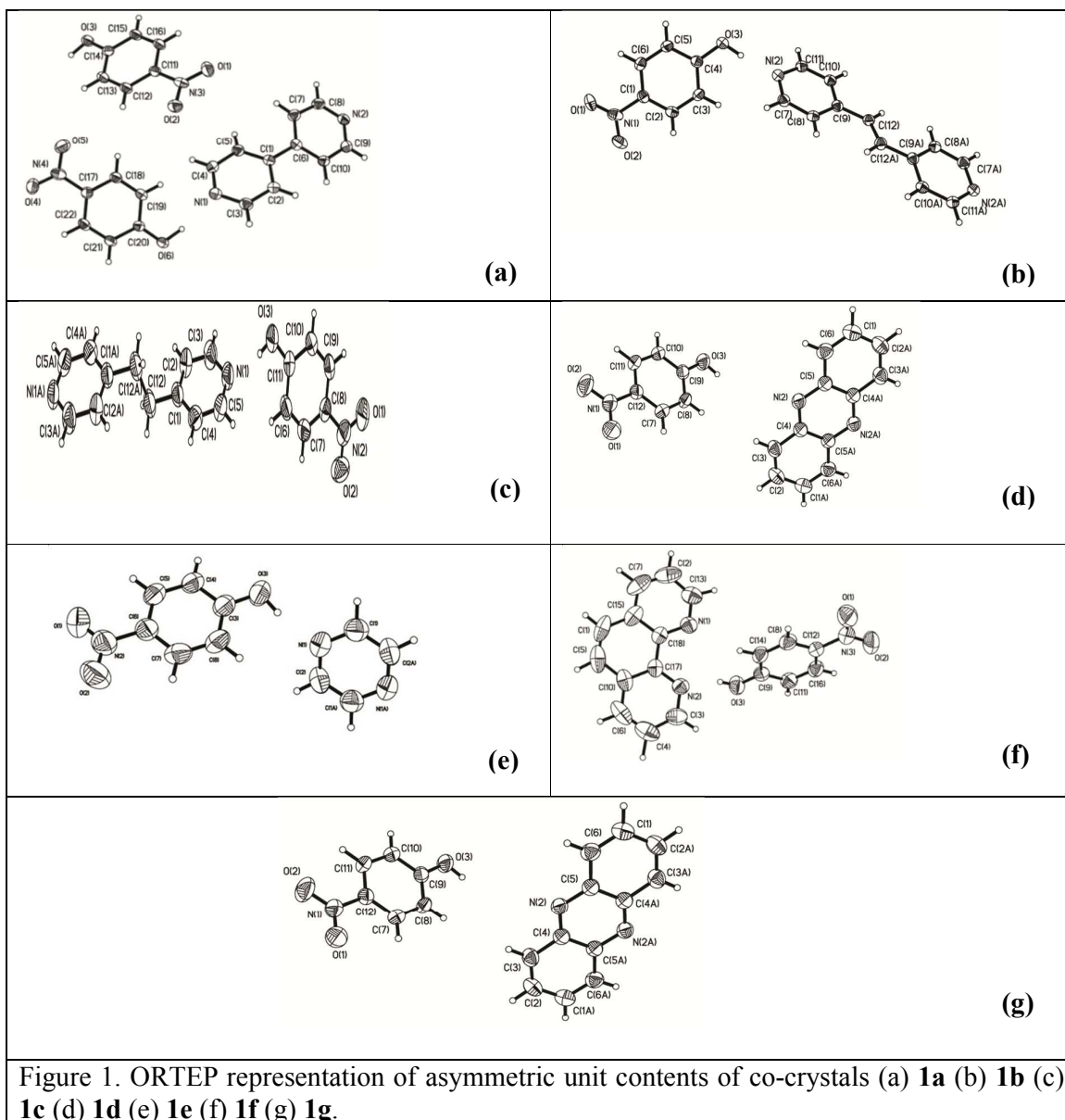
Differential scanning calorimetry (DSC)

Thermal analysis was carried on Perkin-Elmer DSC 8000 instrument. Stainless steel pans were used for the experiment, and the calibration of the instrument was done with the standard sample indium. A sealed empty pan was used as reference pan and samples were heated under a nitrogen atmosphere at a scan rate of $10^\circ \text{ min}^{-1}$.

RESULTS AND DISCUSSION

Crystal structure analysis of the complexes **1a-1g**.

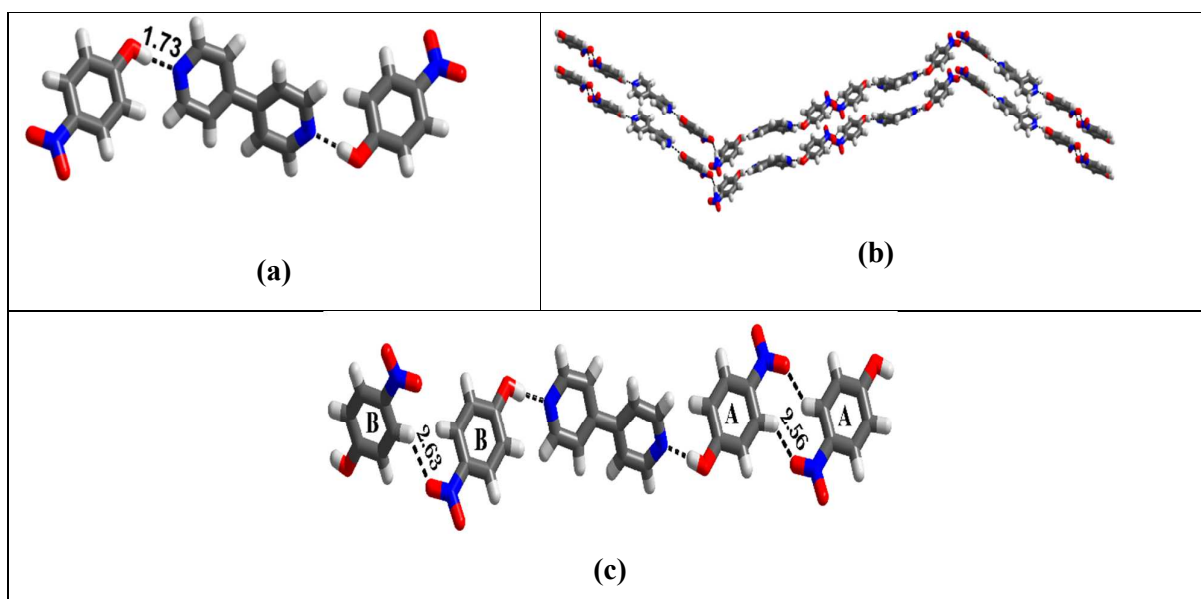
The obtained co-crystals, **1a-1g**, were analysed by Single crystal X-ray diffraction technique and the resultant asymmetric unit contents of all have been shown in Figure 1 in the form of ORTEP.

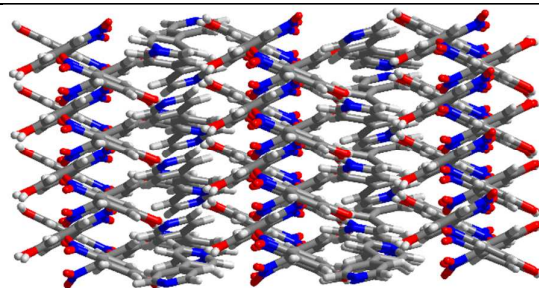


4-nitrophenol and 4,4'-bipyridine, **1a**:

The co-crystal of 4-nitrophenol (**1**) and 4,4'-bipyridine (**a**) were obtained from MeOH by slow evaporation method. Structure determination by single crystal X-ray diffraction method reveals that crystal lattice has an asymmetric unit of **1** and **a** in a 2:1 ratio. ORTEP of the contents of asymmetric unit is shown in Figure 1a. Important and pertinent structure determination parameters are listed in Table 5. Packing analysis reveals that the molecular

1
2
3 recognition between the constituent components is established through O-H \cdots N (H \cdots N, 1.73
4 Å) hydrogen bonds, forming a trimeric unit comprised of one pyridyl molecule and two
5 phenolic moieties (Figure 2a). The trimeric units extend further in one dimension with the
6 help of C-H \cdots O hydrogen bonds produces a *zig-zag* chain (Figure 2b). Such *zig-zag* chain
7 arises due to two different interaction modes of the nitro groups from two unique phenol
8 molecules present in the asymmetric unit. The one which is labelled as A, interact with other
9 molecule through centrosymmetric dimeric C-H \cdots O hydrogen bonds with the corresponding
10 H \cdots O distances being 2.56 Å (Table 6). In case of other which is labelled as B, the entities are
11 present in two planes, inclined at an angle of 55.39°. Such inclination prevents the formation
12 of centrosymmetric dimeric hydrogen bonds. Thus, a single C-H \cdots O (H \cdots O, 2.63 Å) hydrogen
13 bond is formed between the nitrophenol molecules (Figure 2c). Such one dimensional chains
14 are connected to others through C-H \cdots O hydrogen bonds (H \cdots O, 2.32 Å). It is to note that the
15 chains, interact each other through C-H \cdots O hydrogen bonds as mentioned above, are arranged
16 orthogonal to each other to yield a cross-chain structure in three dimension as shown in
17 Figure 2d.



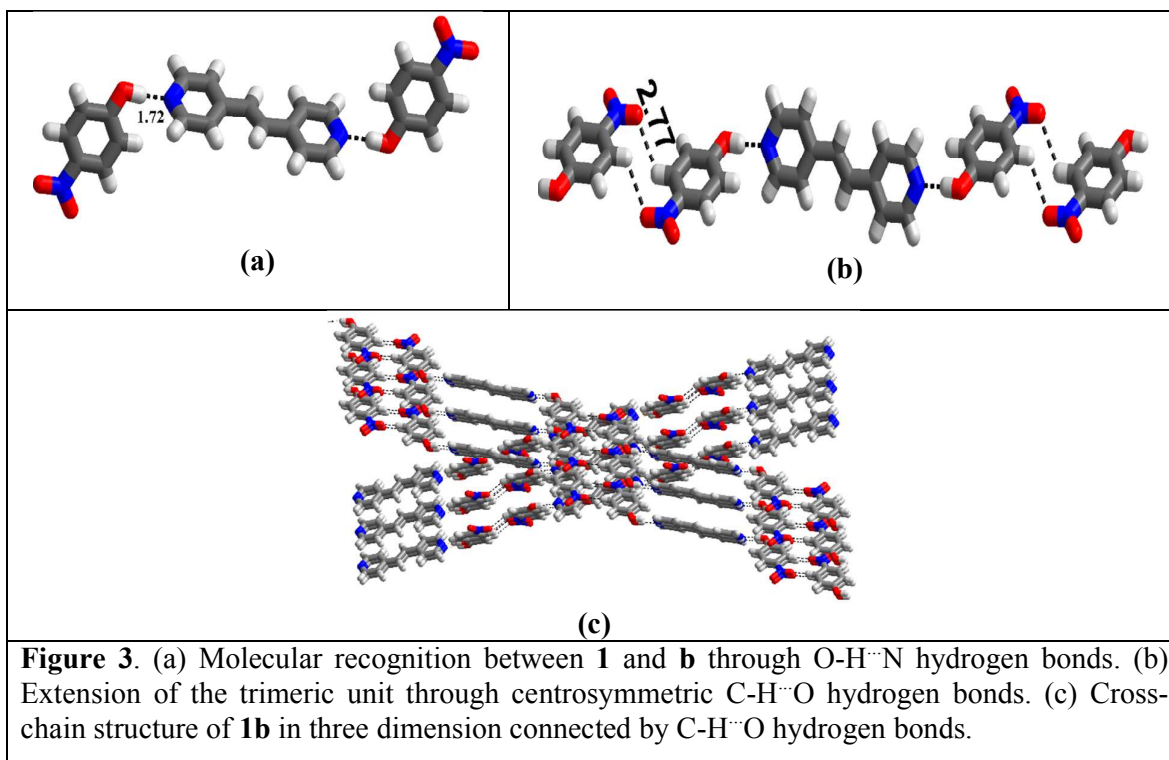


(d)

Figure 2. (a) Molecular interaction between **1** and **a** through O-H...N hydrogen bond. (b) The zig-zag arrangement of chain in **1a**. (c) Dimeric and catemeric C-H...O hydrogen bonds between the nitrophenol molecules in the chain of **1a**. (d) The cross-chain structure of **1a** connected by C-H...O hydrogen bonds.

4-nitrophenol, **1** and 1,2-bis(4-pyridyl)ethene, **1b**:

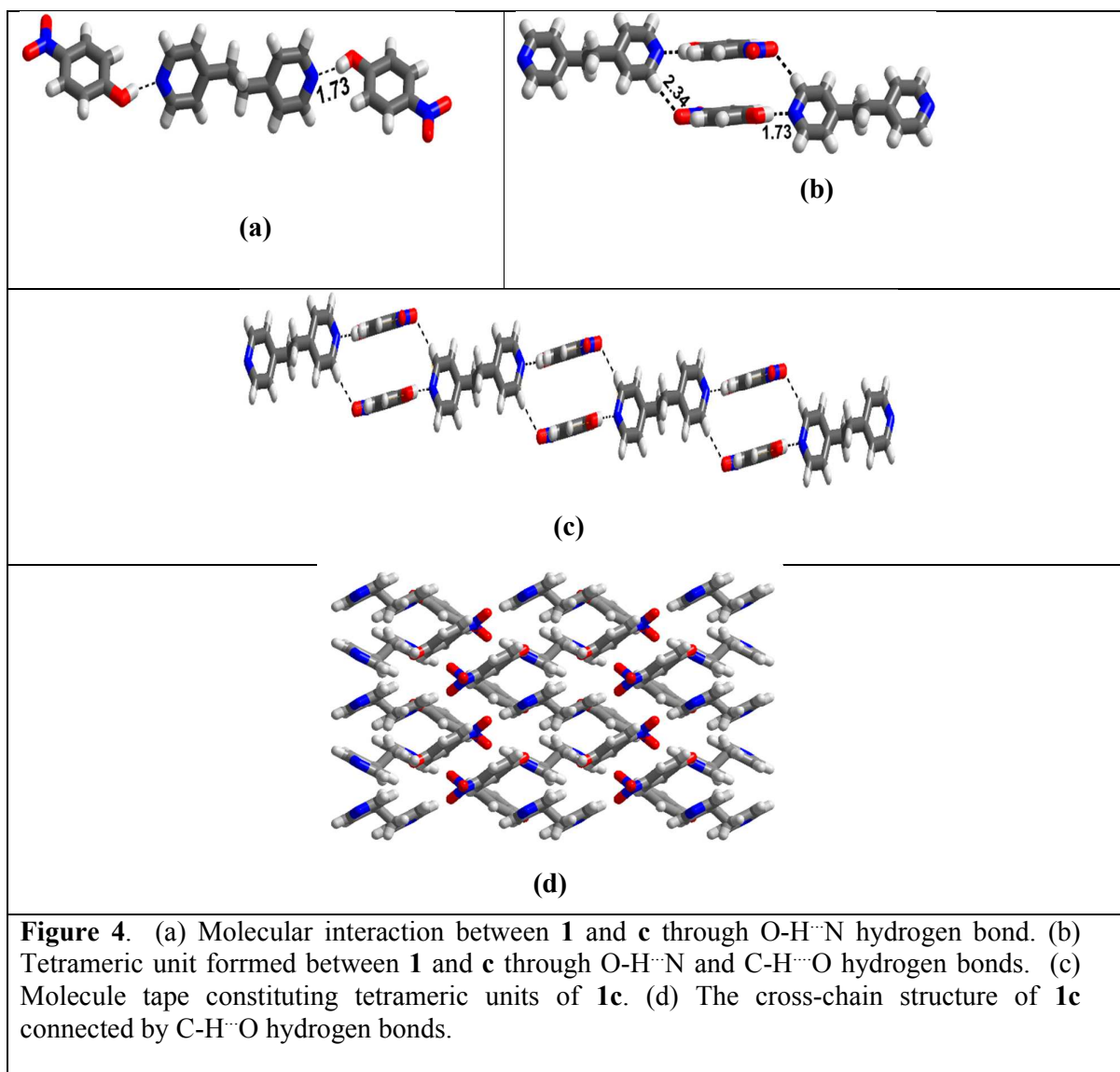
The molecular complex of **1** and 1,2-bis(4-pyridyl)ethene (**b**) obtained from MeOH solution is characterized through single crystal X-ray diffraction method reveals that the co-formers are present in the lattice in a 2:1 ratio of **1** and **b**. The basic recognition between the co-formers, **1** and **b**, has been established through O-H...N (H...N, 1.72 Å) hydrogen bonds leading to a trimeric unit (Figure 3a). These units propagate further through centrosymmetric dimeric C-H...O (H...O, 2.77 Å) hydrogen bonds between the nitro groups to produce the 1-D chains as observed in **1a** (Figure 3b). Such a correlation between **1a** and **1b** may be related to the similarity of the co-formers in both the complexes except for the increased dimension of aza-donor. However, difference in chain arrangements arises due to the twisting of pyridyl group of **a** by 25° with respect to other pyridine unit, whereas, **b** is planar. The chains are crossed as observed in **1a** and form a cross-chain structure in three dimensional arrangement (Figure 3c) with the aid of C-H...O (H...O, 2.60 Å) hydrogen bonds.



4-nitrophenol, **1** and 1,2-bis(4-pyridyl)ethane (**c**), **1c**:

A mixture of **1** and 1,2-bis(4-pyridyl)ethane (**c**) in MeOH on slow evaporation gave good quality crystals. Structure determination by single crystal X-ray diffraction reveals that the co-formers are present in the crystal lattice in a 2:1 ratio of **1** and **c**, respectively. The structural analysis of **1c** shows that the constituent molecules **1** and **c** establish the primary recognition through the O-H \cdots N (H \cdots N, 1.73 Å) hydrogen bonds to yield a trimeric unit as observed in case **1a** and **1b** (Figure 4a). Participation of one of the nitro group oxygen atom in C-H \cdots O (H \cdots O, 2.34 Å) hydrogen bonding with the pyridyl hydrogen atom, results into formation of a tetrameric unit as shown in Figure 4b. Extension of these tetrameric units in one dimension produces molecular tape (Figure 4c) which is different from **1a** and **1b** where the C-H \cdots O hydrogen bond formed between the phenolic units. The interesting feature in three dimensional arrangement of these molecular tapes is that, the pyridyl moieties of the adjacent tapes are flipped by angle of 54.02°. Such deviation from planarity enables the phenolic

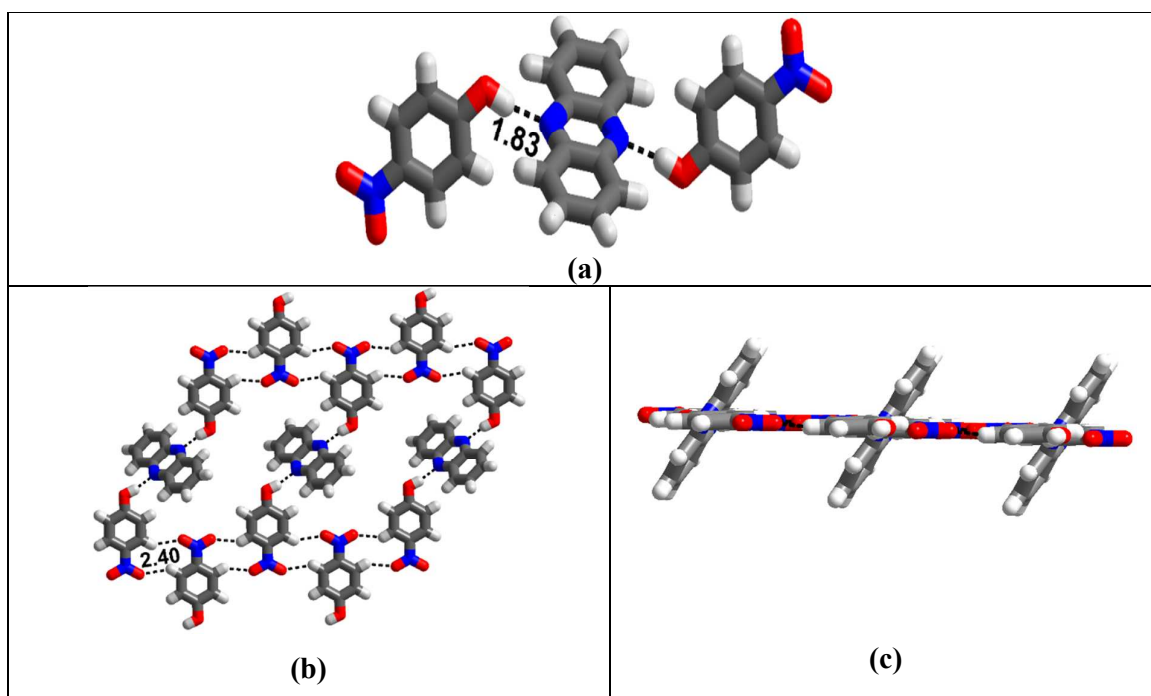
components to utilize the remaining nitro group oxygen atom (which is not participated in tetramer formation) in the formation of C-H \cdots O (H \cdots O, 2.41 Å) hydrogen bonding with the hydrogen atom of the pyridyl group present in the adjacent tape. Such interconnection of tapes gives rise to a crossed tape network (Figure 4d).



4-nitrophenol **1**, and phenazine (d), **1d**:

Towards variation in finding different aza-donor compounds for the preparation of co-crystals with **1**, phenazine has been chosen as the co-former where the nitrogen atom are in

1
2
3 the same ring opposite to each other. The co-crystals prepared between **1** and **d** shows a 2:1
4 molecular complex as represented in form of ORTEP in the Figure 1d. The sterically free
5 nitrogen atoms of the phenazine molecule provide an opportunity of easy approach of
6 phenolic groups to participate in molecular recognition process. The basic recognition
7 between the components is established through O-H \cdots N (H \cdots N, 1.83 Å) hydrogen bonds,
8 resulting into a trimeric unit as shown in Figure 5a. Packing analysis of molecules in the
9 lattice discloses that two-dimensionally the components are arranged in a layer fashion. The
10 analysis of the layers reveals that, the trimeric units enable the phenolic groups to interact
11 with each other through centrosymmetric C-H \cdots O (H \cdots O, 2.40 Å) hydrogen bonds, involving
12 both the oxygen atoms of the -NO₂ group. As a result the phenolic groups are connected to
13 each other and form a chain which are held together by the phenazine molecules (Figure 5b).
14 The intriguing feature of this layer arrangement is that the phenazine moieties are not in the
15 same plane as that of the phenolic chains, rather they inclined to the plane by an angle of
16 56.68° (Figure 5c). Such arrangement of constituent moieties lead to a crossed layer network
17 in three dimension as depicted in Figure 5d.



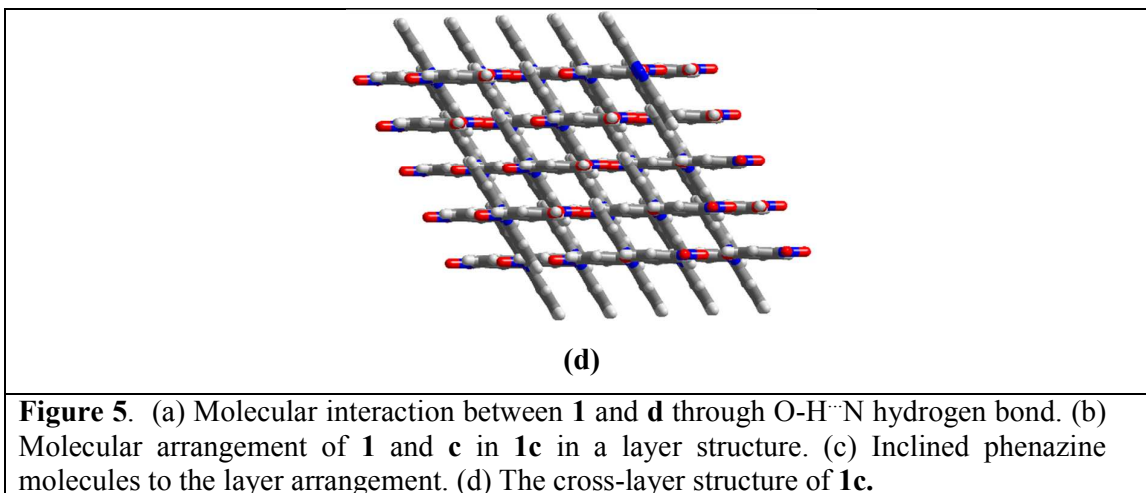
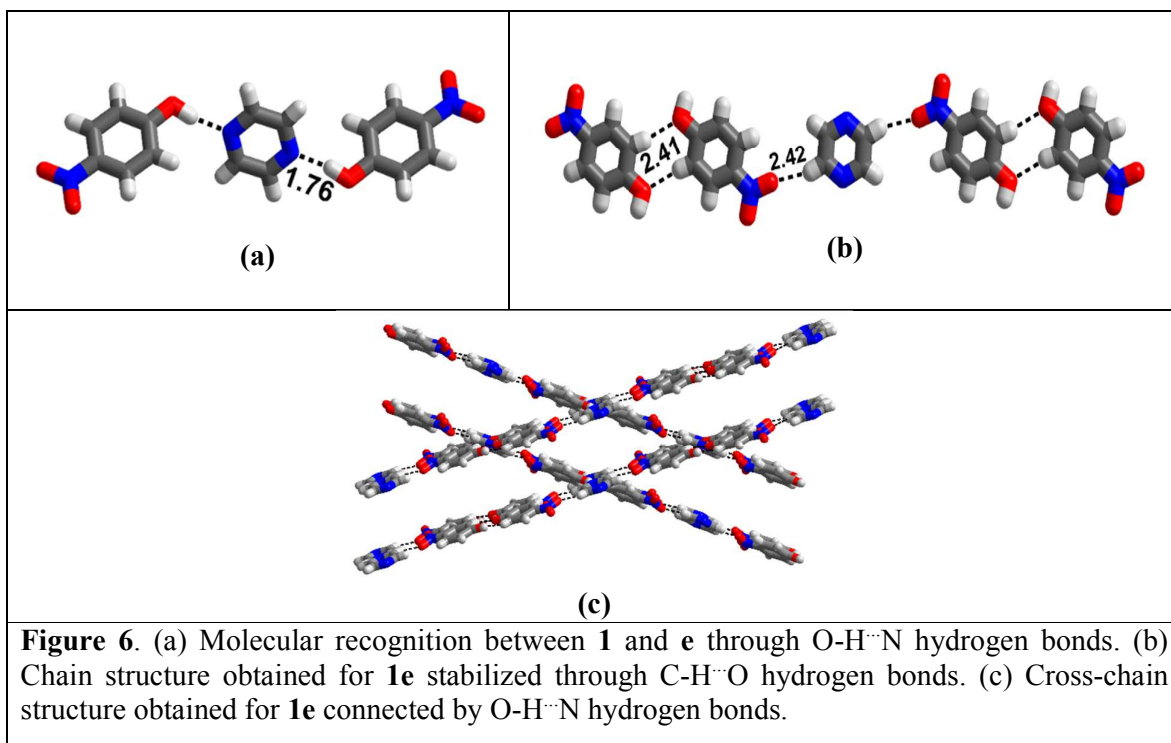


Figure 5. (a) Molecular interaction between **1** and **d** through O-H \cdots N hydrogen bond. (b) Molecular arrangement of **1** and **c** in **1c** in a layer structure. (c) Inclined phenazine molecules to the layer arrangement. (d) The cross-layer structure of **1c**.

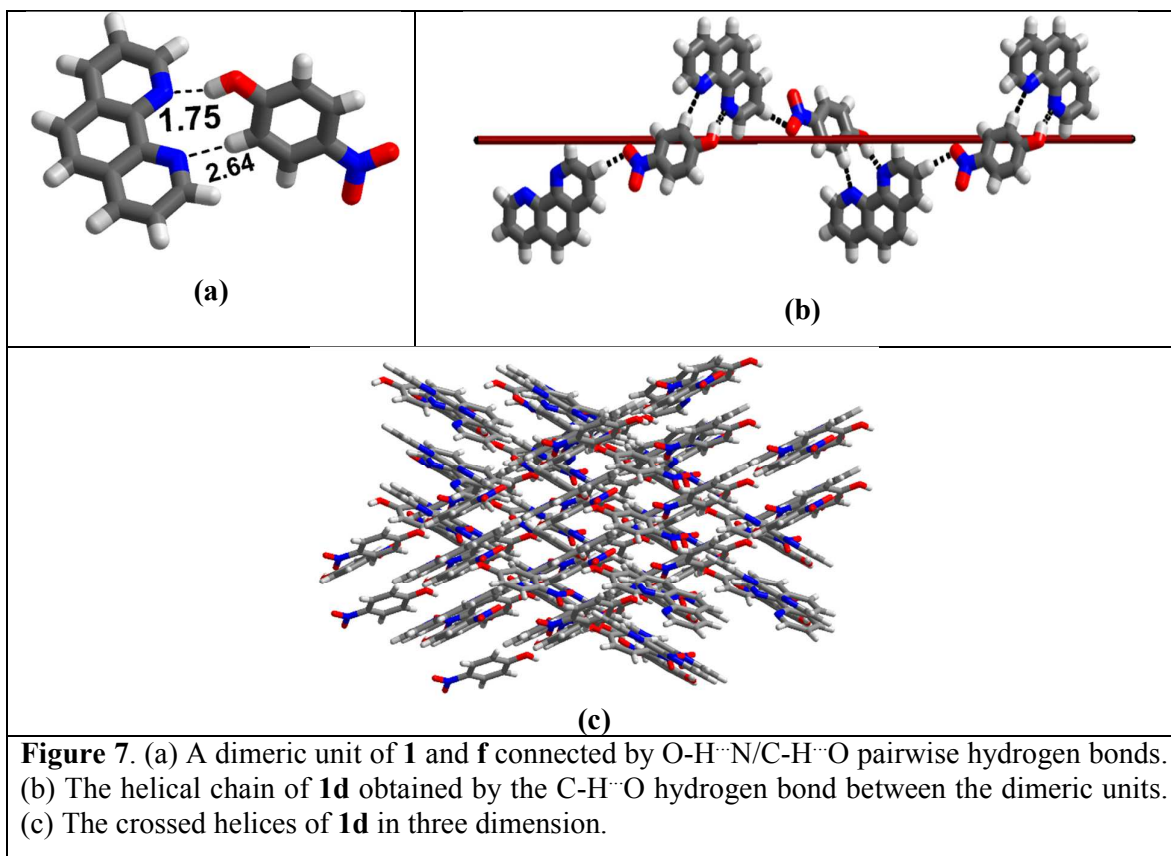
4-nitrophenol, **1**, and pyrazine (**e**), **1e**:

In continuation with aza-donor having the nitrogen opposite in the same ring, we have co-crystallized pyrazine (**e**) with **1** and the single crystal X-ray structural analysis of the co-crystal reveals the components are crystallized in 2:1 ratio of **1** and **e** respectively. The asymmetric unit content of the co-crystal has been illustrated in form of ORTEP as mentioned in Figure 1e. The basic recognition between the components has been achieved through O-H \cdots N (H \cdots N, 1.76 Å) hydrogen bonds, producing a supramolecular motif constituting of two phenolic groups and one pyrazine molecule (Figure 6a). The potentiality of phenolic oxygen to act as hydrogen bond acceptor apart from its donor capability for establishing O-H \cdots N hydrogen bond results into the formation of dimers of phenolic moieties through centrosymmetric C-H \cdots O (H \cdots O, 2.41Å) hydrogen bonds. The dimers thus obtained further propagate through C-H \cdots O (H \cdots O, 2.42Å) hydrogen bonds, established between oxygen atom of the nitro group of **1** and hydrogen atom of **e**, to produce one dimensional chain (Figure 6b). In three dimensions such chains are crossed each other as observed in **1a**, **1b** and **1c** (Figure 6c). However, in case of **1e** the cross-chain interaction is observed through the O-H \cdots N interaction rather than C-H \cdots O hydrogen bonds as noted in **1a**, **1b** and **1c**.



4-nitrophenol, **1** and 1,10-phenanthroline (**f**), **1f**:

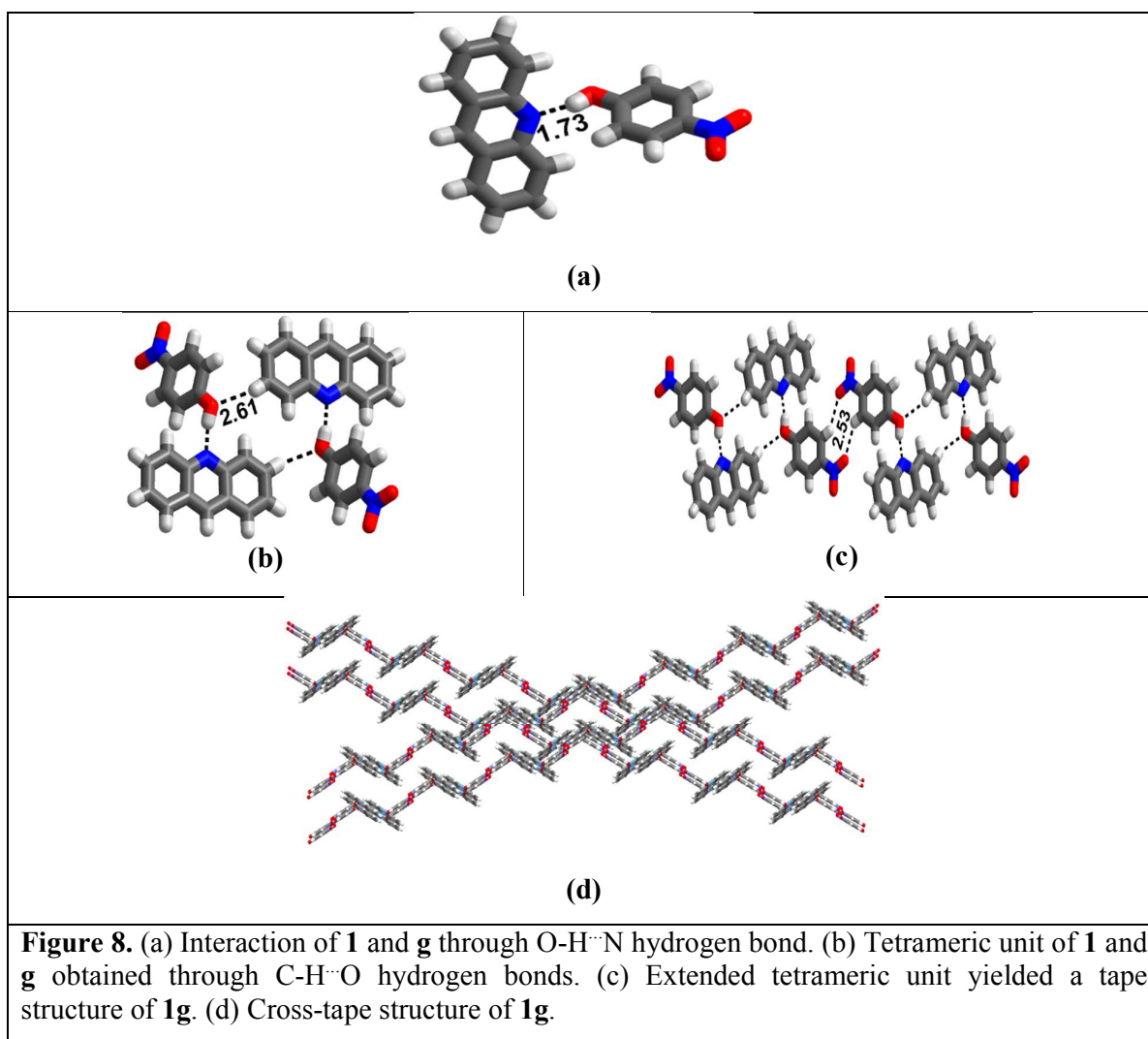
The co-crystal of **1** and 1,10-phenanthroline (**f**) were obtained in the form of single crystals from MeOH. Structure determination reveals formation of a molecular complex of **1** and **f** in a 1:1 ratio unlike in **1a** – **1e**, where it is 2:1. The molecules of **1** interact with **f** through a pair-wise, O-H \cdots N/C-H \cdots N hydrogen bonds with the corresponding H \cdots N distances of 1.75 and 2.64 Å, respectively, producing a dimeric unit (Figure 7a). This is due to the segregation of nitrogen donors on one side **f** which imposes a severe steric hindrance for the approach of two phenolic components. The dimeric ensembles thus produced are further held together by C-H \cdots O (H \cdots O, 2.31 Å) hydrogen bonds, established between pyridyl hydrogen atom and nitro oxygen atom, leading to the formation of a helical arrangement (Figure 7b). Such helices are crossed further with the aid of C-H \cdots O (H \cdots O, 2.54 and 2.67 Å) hydrogen bond by utilizing both nitro and phenolic oxygen atoms to yield a cross-chain structure as observed in the case of **1a**, **1b** and **1e** (Figure 7c).



4-nitrophenol, **1** and acridine (**g**), **1g**:

The structural analysis of co-crystal of **1** and acridine (**g**) crystallized from methanol shows a 1:1 molecular complex (Figure 1g). The composition is seems to be obvious as the acceptor pyridyl molecule, acridine, has only one binding site nitrogen atom. The constituent molecules participate in molecular recognition phenomena through single O-H...N (H...N, 1.73 Å) hydrogen bond by utilizing the donor phenolic OH group and acceptor pyridyl nitrogen. The basic supramolecular motif thus formed has been illustrated in Figure 8a. The phenolic oxygen atom can accommodate both O-H...N and C-H...O hydrogen bonds by acting as hydrogen bond donor in former and as acceptor in later case. This potentiality of phenolic oxygen atom enables the formation of a tetrameric unit as illustrated in Figure 8b. The nitro group oxygen atom involves in the formation of a centrosymmetric C-H...O (H...O, 2.53 Å), which facilitate propagation of tetrameric units in one dimension in form of molecular tape as

shown in Figure 8c. Such tapes are crossed each other in three dimension to produce a crossed tape arrangement as represented in Figure 8d. However, the crossed tapes are connected by weak van der Waals interactions.



Supramolecular features and melting point behaviour of co-crystals

It is interesting to note that all the co-crystals show a 3-D cross-chain close packed network structure which might reflect in their melting point behaviour. Thus, melting point is determined by Differential Scanning Calorimetry (DSC) and the observations are listed in Table 1. All the co-crystals, **1a-1g**, show higher melting point compared to their respective co-formers. This may be due the strong heteromeric interactions, established between the co-formers in the co-crystals in comparison to their homomeric aggregation in the pure form (supporting information, Figure S2). However solely based on interaction strength the melting point elevation phenomena could not be concluded.

Table 1. Melting point of the co-crystals, **1a – 1g**

Co-Crystal	Co-Crystal m.p. (°C)	Cofomers ^a m.p. (°C)	Difference in m.p. (°C) ^b
1a	164	114/114	50
1b	164	153/114	11
1c	153	110/114	30
1d	183	177/114	6
1e	117	52/114	3
1f	154	117/114	37
1g	132	110/114	18

^aFirst value is the m.p. of the respective aza-donor in the co-crystal, while the second value is for the 4-nitrophenol. ^bDifference is calculated between the co-crystal and higher melting point co-former.

Correlation of melting point trend among the co-crystals reported here would be difficult due to the structural diversity among the aza-compounds. However, we have attempted to corroborate the melting point behaviour by grouping the aza-compounds based on the positions of nitrogen atoms. Thus, **a**, **b** and **c** are clustered in one group (I) wherein the pyridyl units are separated by covalent bond(s). While **d** and **e** are placed in second group (II) because of rigid conformation of the aza-compounds apart

1
2
3 from the nitrogen atoms are placed in same ring opposite to each other. Although **f** and
4
5 **g** are rigid like **d** and **e**, the acceptor(s) is placed in one side as a result **f** and **g** are
6
7 classified as third group (III) entities. In group I, the aza compounds, **a**, **b** and **c**,
8
9 exhibit crossed chain network structures of varied degree of entanglement as depicted
10
11 in Figure 2d, 3c and 4d. Such variation in structure can be explained based on the 1-D
12
13 structural features of the molecular components which in turn depend upon the
14
15 possibility of twisting of pyridyl groups of aza-compounds. However only **a** shows
16
17 twisting of pyridyl group with the angle of 25° whereas **b** and **c** are collinear and
18
19 parallel respectively. This differentiation in the geometrical features of **a**, **b** and **c** lead
20
21 to the formation of 1-D zig-zag chain (**1a**) (Figure 2b), 1-D planar chain (**1b**) (Figure
22
23 3b) and 1-D planar tape (**1c**) (Figure 4c), which ultimately induce variation in their
24
25 respective 3-D arrangement. **1a** and **1b** with cross-chain structures with close packing
26
27 arrangement show higher melting point of 164°C. However, **1c** shows the melting
28
29 point of 154°C perhaps because of less efficient cross-chain packing arrangement.
30
31
32

33
34 Apart from structural correlation melting point behaviour of the co-crystals, **1a-1c**,
35
36 is further corroborated using packing efficiency and crystal density as listed in Table
37
38 2. The increase in packing efficiency and crystal density is in the order of **1a**≈**1b**>**1c**,
39
40 clearly indicates the higher melting point for **1a** and **1b** compared to **1c**. Apart from
41
42 this total number of possible “strong hydrogen bonds” in the co-crystals is calculated
43
44 because intermolecular interactions are the key component for the aggregation of
45
46 molecular entities in supramolecular assemblies. Thus calculation has been done by
47
48 following the assumption of Veldis et. al. by considering three C-H···O bonds are
49
50 equivalent to one strong O-H···N hydrogen bond³⁴ (Table 6). **1a** and **1b** with almost
51
52 equal “strong hydrogen bonds” shares the melting point; however **1c** with low number
53
54 of strong hydrogen bond shows less melting point compared to **1a** and **1b**.
55
56
57
58
59
60

Table 2. The number of hydrogen bonds, density and packing co-efficient in correlation with melting point of the co-crystals, **1a** – **1c**.

Co-Crystal	Co-Crystal m.p.	Density (gcm ⁻³)	Total Strong hydrogen bonds	Packing Co-efficient (%)
1a	164	1.467	3.33	73.4
1b	164	1.409	3	71.6
1c	153	1.345	1.66	67.8

The three dimensional aggregation of complexes **1d** (Figure 5d) and **1e** (Figure 6c) in group II also exhibit distinguished features with respect to their packing. Phenazine being equipped with extra aromatic rings forms layer arrangement whereas the involvement of ortho hydrogen atoms of pyrazine, devoid of fused aromatic rings forms C-H...O hydrogen bonds results in to chain structure. Such differences in structural features are also reflected in their melting point as phenazine shows higher melting point value compared to that of pyrazine. The melting point behaviour further quantified with consideration of total possible strong hydrogen bonds, packing co-efficiency and co-crystal density as listed in Table 3.

Table 3. Correlation between co-crystal melting point, density, hydrogen bond efficiency and packing co-efficiency of complexes **1d** and **1e**.

Co-Crystal	Co-Crystal m.p.	Density (gcm ⁻³)	Total Strong hydrogen bonds	Packing Co-efficient (%)
1d	183	1.461	3	71.9
1e	117	1.390	2.33	67.6

Co-crystals **1f** and **1g** are grouped together because of their 1:1 stoichiometry. Though in both the cases cross chain networks have been obtained but features of such networks are completely distinguished from each other due to their striking difference in the 1D structure. In case of **1f** 1D helical chain has been obtained whereas 1D molecular tape has been encountered for **1g** (Figure 7b and 8c). These complexes also show linear variation of their

1
2
3 melting points with respect to any of the discussed parameters such as crystal density,
4
5 packing coefficient and number of strong hydrogen bond (Table 4). Higher the value of any
6
7 considered parameter results into elevated melting point of the co-crystal. The higher melting
8
9 point for **1f** could be understood from its structural features as the crossed helical chains of **1f**
10
11 protrude each other for efficient packing through series of C-H \cdots O hydrogen bonds. Thus,
12
13 enhances the density as well as packing coefficient of the complex. In case of **1g**, the
14
15 molecules are arranged as planar tapes and undergo cross-chain structure. It is to note that,
16
17 although **1g** forms a cross-chain structure, the chains are connected only by weak van der
18
19 Waals interactions. Thus, the molecular complex, **1g**, exhibit lower density and packing
20
21 efficiency hence the complex has lower melting point as compared to **1f**.
22
23
24
25

26 **Table 4.** Correlation between co-crystal melting point, density, total number of strong
27 hydrogen bonds and packing co-efficiency of group III complexes.
28

Co-Crystal	Co-Crystal m.p.	Density (gcm ⁻¹)	Total Strong hydrogen bonds	Packing Co-efficient (%)
1f	154	1.424	3	71.3
1g	132	1.389	2	70.4

	1a	1b	1c	1d	1e	1f	1g
formula	2(C ₆ H ₅ NO): (C ₁₀ H ₈ N ₂)	2(C ₆ H ₅ N ₃): (C ₁₂ H ₁₀ N ₂)	2(C ₆ H ₅ NO): (C ₁₂ H ₁₂ N ₂)	2(C ₆ H ₅ N ₃): (C ₁₂ H ₈ N ₂)	2(C ₆ H ₅ N ₃): (C ₄ H ₄ N ₂)	(C ₆ H ₅ NO ₃) : (C ₁₂ H ₈ N ₂)	(C ₆ H ₅ NO): (C ₁₃ H ₉ N)
formula weight	434.40	460.44	462.46	458.42	358.31	319.31	318.32
crystal shape	needle	needle	plate	Needle	needle	plate	plate
crystal colour	pale yellow	pale yellow	colourless	pale yellow	colourless	colourless	colourless
crystal system	monoclinic	monoclinic	monoclinic	Triclinic	monoclinic	orthorhombic	monoclinic
space group	<i>P</i> 2 ₁ / <i>c</i>	<i>P</i> 2 ₁ / <i>c</i>	<i>P</i> 2 ₁ / <i>c</i>	<i>P</i> $\bar{1}$	<i>P</i> 2 ₁ / <i>c</i>	<i>P</i> 2 ₁ 2 ₁	<i>P</i> 2 ₁ / <i>n</i>
<i>a</i> /Å	19.090(4)	12.760(3)	11.642(2)	3.923(2)	10.421(4)	3.916(2)	3.992(1)
<i>b</i> /Å	3.808(1)	3.880(1)	7.386(2)	9.681(5)	7.043(2)	15.758(1)	16.269(5)
<i>c</i> /Å	27.347(1)	22.520(1)	13.509(3)	14.337(8)	12.206(4)	24.138(2)	23.581(6)
α°	90	90	90	76.99(2)	90	90	90
β°	98.38(3)	103.28(3)	100.55(1)	86.28(2)	107.19(1)	90	91.26(1)
γ°	90	90	90	79.09(2)	90	90	90
<i>V</i> /Å ³	1966.8(7)	1085.1(4)	1142.0(4)	520.9(5)	855.8(5)	1489.8(2)	1531.1(7)
<i>Z</i>	4	2	2	1	2	4	4
<i>D_c</i> /g cm ⁻³	1.467	1.409	1.345	1.461	1.390	1.424	1.381
<i>T</i> (K)	296	296	296	296	296	296	296
λ (Mo <i>K</i> α)	0.71073	0.71073	0.71073	0.71073	0.71073	0.71073	0.71073
μ , mm ⁻¹	0.109	0.104	0.099	0.108	0.109	0.100	0.095
2 θ [°]	52.74	52.74	54.99	56.69	53.12	56.49	52.66
<i>F</i> (000)	904	480	484	238	372	664	664
total reflections	15620	4521	22135	19724	21481	34525	10983
unique reflections	5295	2483	2614	2596	1758	3681	2817
no. of parameters	355	194	156	190	147	269	218
<i>R</i> ₁ , I>2 σ (<i>I</i>)	0.0567	0.0454	0.0481	0.0452	0.0493	0.0442	0.0532
<i>WR</i> ₂ , I>2 σ (<i>I</i>)	0.1787	0.1170	0.1457	0.1137	0.1582	0.1011	0.1230
CCDC No.	994011	994013	994012	994015	1426432	994014	1426431

Table 5. Crystallographic information for the co-crystals of **1a-1g**

Table 6. Characterization of hydrogen bond distances (Å) and angles (°) observed in the structures **1a-1g***

H-Bond	1a(bpy)			1b (bpyee)			1c (bpyea)			1d (phenz)			1e (pyrazine)			1f (1,10)			1g (acri)		
O-H...N	1.74	2.72	170	1.72	2.69	175	1.73	2.69	166	1.83	2.80	168	1.76	2.73	167	1.75	2.69	161	1.73	2.69	164
	1.73	2.71	174																		
C-H...O	2.56	3.28	123	2.75	3.45	122	2.41	3.47	167	2.80	3.85	165	2.60	3.51	142	2.31	3.37	165	2.53	3.45	143
	2.54	3.25	122	2.60	3.53	143	2.34	3.41	169	2.73	3.36	116	2.41	3.44	157	2.54	3.35	130	2.61	3.51	140
	2.32	3.37	163	2.54	3.22	120				2.74	3.51	127	2.36	3.44	176	2.78	3.65	138	2.60	3.36	127
	2.46	3.26	130	2.61	3.26	118				2.63	3.43	130	2.42	3.47	161	2.69	3.32	117			
				2.60	3.34	124				2.40	3.31	140	1.76	2.73	167	2.67	3.34	120			
				2.71	3.40	121				2.39	3.29	139									
C-H...N																2.64	3.43	131			

* In each row the three numbers for every structure represent H...A and D...A distances and <D-H...A

CONCLUSIONS

Co-crystals of 4-nitrophenol with various aza-compounds are synthesized and characterized through single crystal X-ray diffraction method. The structural analysis of all the co-crystals shows a close packed arrangement due to cross-chain network structures of the constituent molecules. Thermal analysis of all co-crystals, **1a-1g**, shows higher melting point compared to their respective co-formers and such elevated melting point of the co-crystals may be due to the cross-chain close packed arrangement of the constituent molecules. For ease of understanding of the melting point behaviour, the co-crystals are categorized into three groups based on the conformation and positions of the nitrogen atoms of aza-compounds. Apart from the structural features, the melting point properties of the co-crystals are corroborated with crystal density, packing co-efficient and number of strong hydrogen bonds which infers a linear relationship between the co-crystal melting point and any of these parameters. Thus, in group I **1a** and **1b** show higher melting point compared to **1c**, in group II **1d** is higher than **1e** and in group III **1f** shows higher melting point than **1g**. This study of melting point behaviour of co-crystals of 4-nitrophenol with various aza-compounds would assist the organic material chemist to synthesize materials with high thermal stability.

ASSOCIATED CONTENT

Supporting Information

DSC plots of the complexes

Hirshfeld surface analysis

AUTHOR INFORMATION

Corresponding Author

*E-mail: amrita.nayak003@gmail.com.

Notes

The authors declare no competing financial interest.

ACKNOWLEDGMENTS

We gratefully acknowledge MHRD for financial support.

REFERENCES

1. Arora, K. K.; Pedireddi, V. R. *J. Org. Chem.* **2003**, *68*, 9177-9185.
2. Varughese, S.; Pedireddi, V. R. *Chem. Commun.* **2005**, 1824-1826.
3. Wenger, M.; Bernstein, J. *Mol. Pharm.* **2007**, *4*, 355-359.
4. Delori, A.; Suresh, E.; Pedireddi, V. R. *Chemistry-a European Journal* **2008**, *14*, 6967-6977.
5. Rajput, L.; Biradha, K. *Cryst. Growth Des.* **2009**, *9*, 40-42.
6. Manjare, Y.; Pedireddi, V. R. *Cryst. Growth Des.* **2011**, *11*, 5079-5086.
7. Aitipamula, S.; Chow, P. S.; Tan, R. B. H. *CrystEngComm* **2014**, *16*, 3451-3465.
8. Nagarajan, V.; Pedireddi, V. R. *Cryst. Growth Des.* **2014**, *14*, 4803-4810.
9. Good, D. J.; Rodriguez-Hornedo, N. *Cryst. Growth Des.* **2009**, *9*, 2252-2264.
10. Smith, A. J.; Kavuru, P.; Wojtas, L.; Zaworotko, M. J.; Shytle, R. D. *Mol. Pharm.* **2011**, *8*, 1867-1876.
11. Aitipamula, S.; Vangala, V. R.; Chow, P. S.; Tan, R. B. H. *Cryst. Growth Des.* **2012**, *12*, 5858-5863.
12. Deng, Z.-P.; Huo, L.-H.; Zhao, H.; Gao, S. *Cryst. Growth Des.* **2012**, *12*, 3342-3355.
13. Tao, Q.; Chen, J.-M.; Ma, L.; Lu, T.-B. *Cryst. Growth Des.* **2012**, *12*, 3144-3152.
14. Bolla, G.; Sanphui, P.; Nangia, A. *Cryst. Growth Des.* **2013**, *13*, 1988-2003.
15. Landenberger, K. B.; Bolton, O.; Matzger, A. J. *Angew. Chem. Int. Ed.* **2013**, *52*, 6468-6471.
16. Chattoraj, S.; Shi, L.; Chen, M.; Alhalaweh, A.; Velaga, S.; Sun, C. C. *Cryst. Growth Des.* **2014**, *14*, 3864-3874.
17. Sanphui, P.; Mishra, M. K.; Ramamurty, U.; Desiraju, G. R. *Mol. Pharm.* **2015**, *12*, 889-897.

- 1
2
3 18. Koshima, H.; Miyamoto, H.; Yagi, I.; Uosaki, K. *Cryst. Growth Des.* **2004**, *4*, 807-
4 811.
5
6
7 19. Goroff, N. S.; Curtis, S. M.; Webb, J. A.; Fowler, F. W.; Lauher, J. W. *Org. Lett.*
8 **2005**, *7*, 1891-1893.
9
10
11 20. Sokolov, A. N.; Friščić, T.; MacGillivray, L. R. *J. Am. Chem. Soc.* **2006**, *128*, 2806-
12 2807.
13
14
15 21. He, G.; Jacob, C.; Guo, L.; Chow, P. S.; Tan, R. B. H. *The Journal of Physical*
16 *Chemistry B* **2008**, *112*, 9890-9895.
17
18
19
20 22. Sarma, B.; Reddy, L. S.; Nangia, A. *Cryst. Growth Des.* **2008**, *8*, 4546-4552.
21
22
23 23. Shattock, T. R.; Arora, K. K.; Vishweshwar, P.; Zaworotko, M. J. *Cryst. Growth Des.*
24 **2008**, *8*, 4533-4545.
25
26
27 24. Desiraju, G. R. *Cryst. Growth Des.* **2011**, *11*, 896-898.
28
29
30 25. Sanphui, P.; Devi, V. K.; Clara, D.; Malviya, N.; Ganguly, S.; Desiraju, G. R. *Mol.*
31 *Pharm.* **2015**, *12*, 1615-1622.
32
33
34 26. Ghosh, S.; Mishra, M. K.; Ganguly, S.; Desiraju, G. R. *J. Am. Chem. Soc.* **2015**, *137*,
35 9912-9921.
36
37
38 27. Ghosh, S.; Mishra, M. K.; Kadambi, S. B.; Ramamurty, U.; Desiraju, G. R. *Angew.*
39 *Chem.* **2015**, *127*, 2712-2716.
40
41
42 28. Aakeröy, C. B.; Forbes, S.; Desper, J. *J. Am. Chem. Soc.* **2009**, *131*, 17048-17049.
43
44
45 29. Callear, S. K.; Hursthouse, M. B.; Threlfall, T. L. *CrystEngComm* **2010**, *12*, 898-908.
46
47
48 30. Katritzky, A. R.; Jain, R.; Lomaka, A.; Petrukhin, R.; Maran, U.; Karelson, M. *Cryst.*
49 *Growth Des.* **2001**, *1*, 261-265.
50
51
52 31. Dunitz, J. D.; Gavezzotti, A. *Angew. Chem. Int. Ed.* **2005**, *44*, 1766-1787.
53
54
55 32. Braga, D.; Dichiarante, E.; Palladino, G.; Grepioni, F.; Chierotti, M. R.; Gobetto, R.;
56 Pellegrino, L. *CrystEngComm* **2010**, *12*, 3534-3536.
57
58
59
60

- 1
2
3 33. Bond, A. D. *CrystEngComm* **2006**, *8*, 333-337.
4
5 34. Orola, L.; Veidis, M. V.; Mutikainen, I.; Sarcevic, I. *Cryst. Growth Des.* **2011**, *11*,
6
7 4009-4016.
8
9 35. Fleischman, S. G.; Kuduva, S. S.; McMahon, J. A.; Moulton, B.; Bailey Walsh, R. D.;
10
11 Rodríguez-Hornedo, N.; Zaworotko, M. J. *Cryst. Growth Des.* **2003**, *3*, 909-919.
12
13 36. Childs, S. L.; Chyall, L. J.; Dunlap, J. T.; Smolenskaya, V. N.; Stahly, B. C.; Stahly,
14
15 G. P. *J. Am. Chem. Soc.* **2004**, *126*, 13335-13342.
16
17 37. Childs, S. L.; Rodriguez-Hornedo, N.; Reddy, L. S.; Jayasankar, A.; Maheshwari, C.;
18
19 McCausland, L.; Shipplett, R.; Stahly, B. C. *CrystEngComm* **2008**, *10*, 856-864.
20
21 38. Stanton, M. K.; Bak, A. *Cryst. Growth Des.* **2008**, *8*, 3856-3862.
22
23 39. Basavoju, S.; Boström, D.; Velaga, S. *Pharm. Res.* **2008**, *25*, 530-541.
24
25 40. Basavoju, S.; Boström, D.; Velaga, S. P. *Cryst. Growth Des.* **2006**, *6*, 2699-2708.
26
27 41. McNamara, D.; Childs, S.; Giordano, J.; Iarriccio, A.; Cassidy, J.; Shet, M.; Mannion,
28
29 R.; O'Donnell, E.; Park, A. *Pharm. Res.* **2006**, *23*, 1888-1897.
30
31 42. Bhatt, P. M.; Ravindra, N. V.; Banerjee, R.; Desiraju, G. R. *Chem. Commun.* **2005**,
32
33 1073-1075.
34
35 43. Vishweshwar, P.; Nangia, A.; Lynch, V. M. *Cryst. Growth Des.* **2003**, *3*, 783-790.
36
37 44. Walsh, R. D. B.; Bradner, M. W.; Fleischman, S.; Morales, L. A.; Moulton, B.;
38
39 Rodríguez-Hornedo, N.; Zaworotko, M. J. *Chem. Commun.* **2003**, 186-187.
40
41 45. Schultheiss, N.; Newman, A. *Cryst. Growth Des.* **2009**, *9*, 2950-2967.
42
43 46. Spek, A. L. *PLATON, Molecular Geometry Program*; University of Utrecht: Utrecht,
44
45 The Netherlands, 1995.
46
47 47. Macrae, C. F.; Bruno, I. J.; Chisholm, J. A.; Edgington, P. R.; McCabe, P.; Pidcock, E.;
48
49 Rodríguez-Monge, L.; Taylor, R.; van de Streek, J.; Wood, P. A. *J. Appl. Cryst.* **2008**, *41*,
50
51 466-470.
52
53
54
55
56
57
58
59
60

1
2
3 48. *Diamond: Crystal and Molecular Structure Visualization*, version 3.1f; Crystal Impact:
4
5 Bonn, Germany, 2008.
6
7
8
9
10
11
12
13
14
15
16
17
18
19
20
21
22
23
24
25
26
27
28
29
30
31
32
33
34
35
36
37
38
39
40
41
42
43
44
45
46
47
48
49
50
51
52
53
54
55
56
57
58
59
60

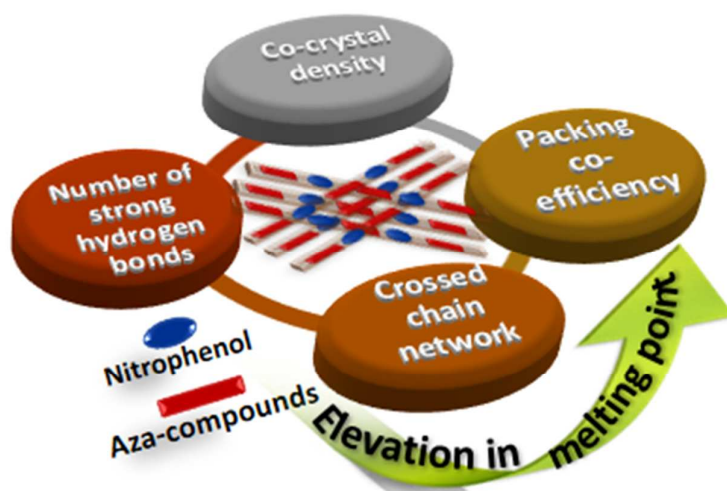
For Table of Contents Use Only

Rational Analysis of Melting Point Behaviour of Co-crystals of Nitrophenol with Some Aza-compounds

Amrita Nayak* and V. R. Pedireddi

Solid State and Supramolecular Structural Chemistry Laboratory, School of Basic Sciences, Indian Institute of Technology Bhubaneswar, Bhubaneswar 751 007, India.

Email: amrita.nayak003@gmail.com



Co-crystals of 4-nitrophenol with various aza-compounds exhibits higher melting point compared to their respective co-formers. Such thermal behaviour linearly correlated with various parameters such as the cross-chain supramolecular architectures, co-crystal density, packing co-efficiency and number of strong hydrogen bonds.